

Effect of Annealing Temperature on the Complex Permeability of $(\text{Fe}_{0.95}\text{Co}_{0.05})_{73.5}\text{Cu}_1\text{Nb}_3\text{Si}_{13.5}\text{B}_9$ Nanocrystalline Amorphous Ribbon

Ratan Krishna Howlader, Sujit Kumer Shil*, Shibendra Shekher Sikder and Dilip Kumar Saha

Department of Physics, Khulna University of Engineering & Technology, Khulna, Bangladesh

Research Article

Received: 18/10/2017

Accepted: 06/11/2017

Published: 12/11/2017

*For Correspondence

Sujit Kumer Shil, Department of Physics,
Khulna University of Engineering & Technology,
Khulna, Bangladesh, Tel: 880-1921090502;

Email: sujitphy.kuet@gmail.com

Keywords: Annealing temperature, Grain size,
Complex permeability, Relative quality factor

ABSTRACT

FINEMET-like amorphous ribbon of composition $(\text{Fe}_{0.95}\text{Co}_{0.05})_{73.5}\text{Cu}_1\text{Nb}_3\text{Si}_{13.5}\text{B}_9$ was prepared by rapid quenching method in an Argon (Ar) atmosphere. The alloy has been annealed in a controlled way in the temperature range of 550 to 750 °C for 30 minutes. Nanocrystalline state was evaluated by X-ray diffraction (XRD). In the range of annealing temperature (T_a), the grain size has been found in the range of 9-26 nm. Frequency dependence of permeability of amorphous and nanocrystalline toroid shaped samples have been measured. The low frequency initial permeability for the optimum annealed samples has been found to 5.8×10^3 and the highest value of quality factor is found for the sample annealed at 550 °C; which also indicates the best heat treatment temperature.

INTRODUCTION

Over the past several decades, amorphous and most recently, research interest in nanocrystalline soft magnetic alloys has dramatically increased. Soft magnetic materials face demanding requirements for high performance electronic and power distribution systems. With the reduction of size into nanometer range, the materials exhibit interesting properties including physical, chemical, magnetic and electrical properties compare to conventional coarse grained counterparts. Soft magnetic nanostructured materials have a number of potential technological applications [1-11]. Nanocrystalline soft magnetic materials were first reported in 1988 by Yoshizawa et al. [12] through controlled crystallization of *Fe-Si-B* amorphous alloys with the addition of copper (*Cu*) and niobium (*Nb*). The development of nanocrystalline *Fe-Si-B-Nb-Cu* alloys, commercially known as FINEMET, established a new approach to develop soft magnetic materials. The nanocrystalline state is achieved by subsequent heat treatment from their as cast amorphous precursor above the primary crystallization temperature. Excellent soft magnetic properties can be found in nanocrystalline materials of *Fe-Si-B* amorphous ribbons containing *Cu* and *Nb*. The addition of *Cu* and *Nb* results in the formation of an ultra-fine grain structure. The main purpose of this research is to determine empirically the optimum annealing temperature, corresponding to maximum permeability, constancy of permeability and maximum frequency range over which the sample can be used as a soft magnetic material.

MATERIALS AND METHODS

The amorphous ribbon with a composition $(\text{Fe}_{0.95}\text{Co}_{0.05})_{73.5}\text{Cu}_1\text{Nb}_3\text{Si}_{13.5}\text{B}_9$ was prepared from high purity *Fe* (99.9%), *Co* (99.9%), *Nb* (99.9%), *Si* (99.9%), *Cu* (99.9%) and *B* (99.9%). The ribbons were produced in an arc furnace on a water-cooled copper hearth by a single roller melt-spinning technique under an atmosphere of pure *Ar* at the Centre of Materials Science, National University of Hanoi, Vietnam. The wheel velocity was about 34 m/s. The ribbons were annealed in a vacuum heat treatment furnace at 550, 600, 625, 650, 675, 700, 725 and 750 °C respectively for constant time 30 minutes and then cooled down to the room temperature. Amorphousness of the ribbon and nanocrystalline structure has been observed by XRD (Philips (PW 3040) X 'Pert PRO XRD) with *Cu-K α* radiation. Lattice parameter (a_0) were calculated using equations $2d \sin \theta = \lambda$ and $a_0 = d\sqrt{2}$, where $\lambda = 1.54178 \text{ \AA}$ for *Cu-K α* radiation. Grain size (D_g) of all annealed samples of the alloy composition has been determined using Debye-Scherrer method [13]. Si contents were calculated using the equation: $X = \frac{(a_0 - 2.8812)}{0.0022}$, where X is at.% Si in the nanograins. The

frequency characteristics i.e. the initial permeability spectra of the toroid shaped samples were measured using an impedance analyzer (model no. 6500B) at room temperature in the frequency range 1 kHz to 13 MHz. The real part of complex permeability (μ') was calculated using relation, $\mu' = L/L_0$, where L is the self-inductance of the sample and L_0 is the inductance of the coil of same geometric shape of vacuum. L_0 is determined using the relation, $L_0 = \mu_0 N^2 S / \pi d$, where μ_0 is the permeability of the free space, N is the number of turns (here $N=10$), S is the area of cross-section $n = \frac{m}{\pi \rho d}$, where m is the weight of the ribbon, d and ρ are the mean diameter and density of the sample. The imaginary part of complex permeability (μ'') was determined using the formula $\mu'' = \mu' \times D$. The relative quality factor was calculated from the Loss factor, $\tan \delta$ ($\tan \delta = \mu'' / \mu'$) using the relation $\mu' Q = \mu' / \tan \delta$.

RESULTS AND DISCUSSION

XRD

XRD spectra of as-cast and annealed at 550 to 750 °C for 30 minutes have been presented in **Figure 1**. One broad peak at $2\theta=45^\circ$ for the as-cast sample confirms the amorphous state. XRD pattern clearly indicates the formation of bcc α -FeCo(Si) phase at $T_a=550^\circ\text{C}$ or above with the appearance of (110), (200) and (211) fundamental diffraction peaks. With the increase of T_a , (110) peak becomes sharper which means the grains are growing bigger. From the **Figure 1** it is also observed that just before (110) peak, another diffraction line with small peak at $2\theta \approx 44^\circ$ appeared for the samples annealed at 700 to 750 °C. This diffraction peak has been matched with Fe_{23}B_6 phase (boride phase).

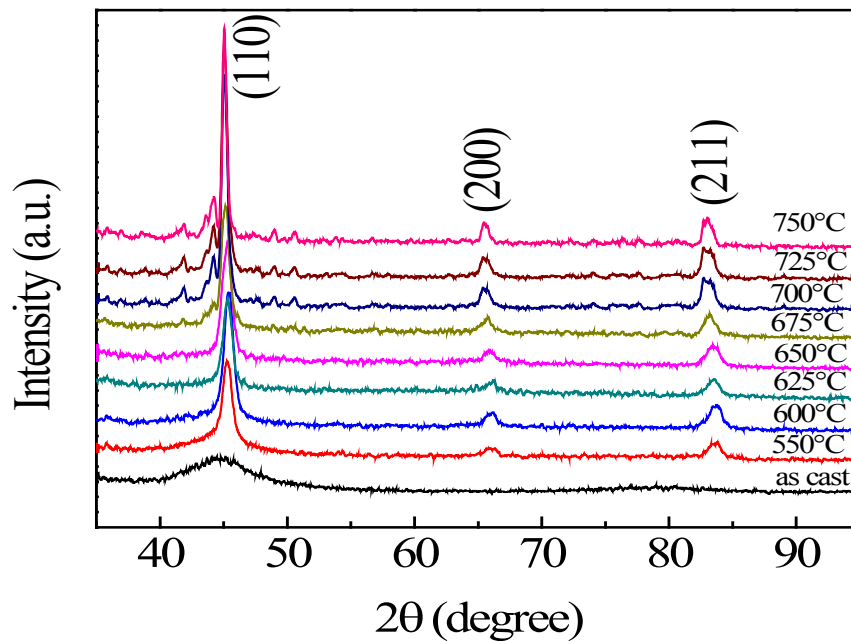


Figure 1. XRD patterns of $(\text{Fe}_{0.95}\text{Co}_{0.05})_{73.5}\text{Cu}_1\text{Nb}_3\text{Si}_{13.5}\text{B}_9$ alloy for as cast and annealed at different temperatures for 30 minutes.

This is because, with increasing T_a the diffusion of Si into α -FeCo space lattice increases and hence increases the formation of α -FeCo(Si) nanograin. At higher T_a , Si diffuses out of nanograins due to recrystallization corresponding to formation of boride phase which is consistent with the result of other FINEMET's [14]. Absence of boride phase in the XRD spectra is possibly due to very small volume fraction of Fe_{23}B_6 . **Figure 2** shows the variation of D_g of α -FeCo(Si) phase with T_a . Enhancement of D_g with T_a complies with the reported result [15]. All the results of θ , d -values, $FWHM$, a_0 , D_g and Si-content from XRD analysis are listed in **Table 1**.

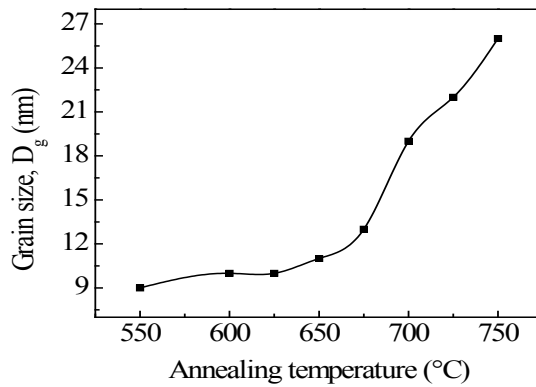


Figure 2. Variation of grain size with annealing temperature of $(Fe_{0.95}Co_{0.05})_{73.5}Cu_1Nb_3Si_{13.5}B_9$ alloy.

T_a (°C)	θ (degree)	d (Å)	a (Å)	FWHM	Si (at%)	D_g (nm)
550	22.6188	2.0044	2.8347	0.93	21.14	9
600	22.6343	2.0031	2.8328	0.83	22	10
625	22.6438	2.0023	2.8317	0.81	22.5	10
650	22.6355	2.0030	2.8327	0.75	22.05	11
675	22.6021	2.0058	2.8367	0.69	20.23	13
700	22.5701	2.0085	2.8404	0.45	18.55	19
725	22.5145	2.0132	2.8471	0.41	15.5	22
750	22.4791	2.0162	2.8514	0.33	13.55	26

Table 1. The values of θ , d -values, a , $FWHM$, Si-content and D_g with respect to T_a of $(Fe_{0.95}Co_{0.05})_{73.5}Cu_1Nb_3Si_{13.5}B_9$ alloy.

Complex Permeability

Figure 3 shows the frequency dependence of the μ' for as-cast and the samples annealed at temperature 550 to 700 °C for a constant annealing time of 30 minutes. From the figure it is observed that the low frequency value of μ' increases with the increase of T_a and attains the maximum value at 550 °C. A sharp increase of μ' is found due to crystallization of α -FeCo(Si) phase. When the T_a is higher than 550 °C, μ' decreases rapidly. At higher T_a , the decrease of μ' may be attributed to the stress developed in the amorphous matrix by growing crystallites. The newly grown crystallites serve as pinning centers at which domain walls are pinned and creates obstructions for their mobility resulting in a decrease in μ' . The evolution of boride phases and the nonmagnetic fcc phases including Cu clusters leads to the increase of magnetocrystalline anisotropy to a high value, as a result of which magnetic hardening takes place [16]. The general characteristic of the curve is that μ' remains fairly constant up to some critical frequency characterized by the onset of resonance connected with the loss component. At critical frequencies, μ' drops rapidly.

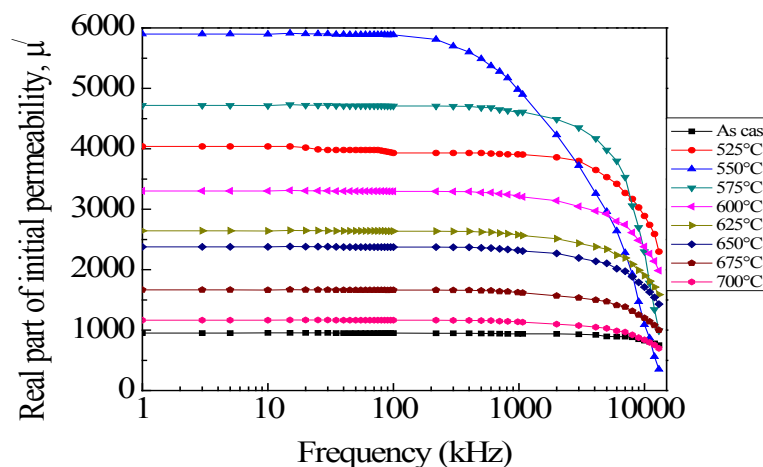


Figure 3. Frequency dependent real part of complex initial permeability of $(Fe_{0.95}Co_{0.05})_{73.5}Cu_1Nb_3Si_{13.5}B_9$ alloy for as-cast and annealed at different temperatures.

The frequency dependent imaginary part of the complex initial permeability (μ'') annealed at different temperatures at constant annealing time 30 minutes are shown in **Figure 4**. These results are quite complimentary to the results of the real part of the complex permeability of samples. After critical frequencies the μ'' increases with increasing frequency. The high value of μ'' for the samples corresponds to high loss factor as shown in **Figure 3**. The origin of the loss factor can be attributed to various domain effects ^[17], which include non-uniform and non-repetitive domain wall motion, domain wall bowing, localized variation of flux densities and nucleation and annihilation of domain walls.

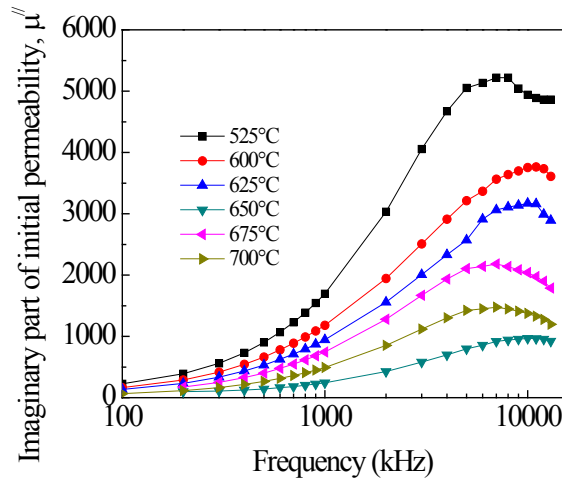


Figure 4. Frequency dependence of imaginary part of complex permeability of $(Fe_{0.95}Co_{0.05})_{73.5}Cu_1Nb_3Si_{13.5}B_9$ alloy annealed at different temperatures.

Relative Quality Factor

The frequency dependence of relative quality factor (μ'/Q) of the sample annealed at different temperatures is shown in **Figure 5**. From the figure it is observed that the μ'/Q initially rises with increasing frequency and reaches a peak value. Beyond the peak value, the μ'/Q is found to decrease. It is also found that the μ'/Q increases with the increase of T_a up to 550°C and with further increase of T_a the μ'/Q decreases. At high frequency, the flux penetration becomes low, as a result the loss is mainly controlled by interaction between the grains of the alloy but at very low frequency the loss is controlled by hysteresis losses. The decrease of μ'/Q with increasing T_a after 550°C is due to increase of D_g for the precipitation of Fe borides ^[16]. The precipitation of very small percent of particles increases the high frequency losses. The highest value of μ'/Q is found for the sample annealed at 550°C, which also indicates the best heat treatment temperature. From all curves, it is noted that the higher values of the μ'/Q in general lie within the frequency range of 10 kHz to 100 kHz. Thus the frequency range for application area might be chosen.

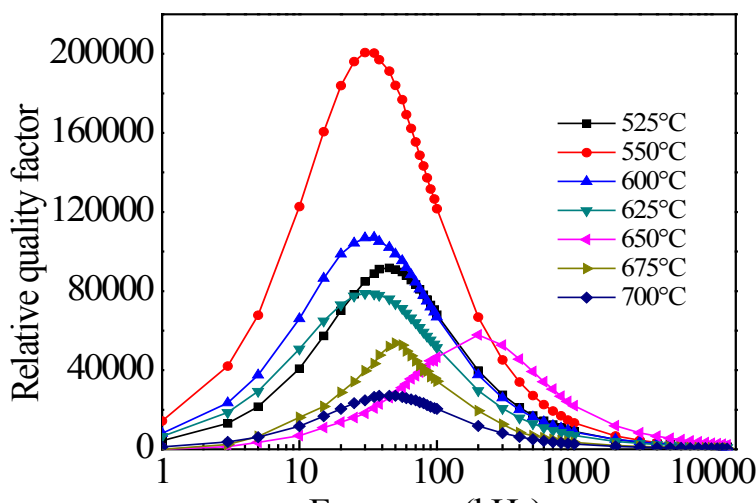


Figure 5. Frequency dependence of relative quality factor of $(Fe_{0.95}Co_{0.05})_{73.5}Cu_1Nb_3Si_{13.5}B_9$ alloy annealed at different temperatures.

CONCLUSION

Nanocrystalline amorphous ribbon of the FINEMET family with a nominal composition $(Fe_{0.95}Co_{0.05})_{73.5}Cu_1Nb_3Si_{13.5}B_9$ has been studied. The amorphous state of the as-cast amorphous ribbons has been confirmed by XRD. The evolution of nanocrystallites of α -FeCo(Si) with T_a have been confirmed from the fundamental diffraction peaks. The grain size of the sample was found from 9 to 26 nm. The maximum μ' is observed for the sample annealed at 550 °C. A sharp increase of μ' at this temperature is due to the formation of nanometric α -FeCo(Si) grain. The highest value of μ'/Q is achieved for the sample annealed at 550 °C in the frequency range 10 kHz to 100 kHz. So, 550 °C is the most suitable heat treatment temperature from the application point of view in case of the present alloy as a soft magnetic material.

ACKNOWLEDGEMENTS

We are grateful to Bangladesh Council for Scientific and Industrial Research (BCSIR) and Materials Science Division, Atomic Energy Centre, Dhaka (AECD) for giving experimental facilities and cordial co-operations.

REFERENCES

1. Kulik T, et al. Correlation between structure and the magnetic properties of amorphous and nanocrystalline $Fe_{73.5}Cu_1Nb_3Si_{13.5}B_9$ alloys. J Magn Magn Mater 1994;133:310-313.
2. Miguel C, et al. Magnetoimpedance of stress and/or field annealed $Fe_{73.5}Cu_1Nb_3Si_{15.5}B_7$ amorphous and nanocrystalline ribbon. J Magn Magn Mater 2003;254-255:463-465.
3. Chen J and Zhu Z. The study on surface chemical modification of $Fe_{71.5}Cu_1Nb_3Si_{13.5}B_9V_2$ amorphous alloy ribbons and its piezomagnetic effect. J Magn Magn Mater 2016;419:451-455.
4. Yapi Liu, et al. Microstructure and magnetic properties of soft magnetic cores of amorphous and nanocrystalline alloys. J Magn Magn Mater 2013;330:119-133.
5. Trilochan Sahoo, et al. Improved magnetoimpedance and mechanical properties on nanocrystallization of amorphous $Fe_{68.5}Si_{18.5}Cu_1Nb_3B_9$ ribbons. J Magn Magn Mater 2013;343:13-20.
6. Partha Sarkar, et al. Magneto-Impedance behavior of Co-Fe-Nb-Si-B based ribbons. J Magn Magn Mater 2010;322:1026-1031.
7. Hossain MK. Development of Nanostructure Formation of $Fe_{73.5}Cu_1Nb_3Si_{13.5}B_9$ Alloy from Amorphous State on Heat Treatment. World J Nano Sci Eng 2015;5:107-114.
8. Kane SN, et al. Effect of quenching rate on crystallization in $Fe_{73.5}Si_{13.5}B_9Cu_1Nb_3$ alloy. J Magn Magn Mater 2000;215-216:372-374.
9. El Ghannami M, et al. Influence of the Preparation Condition on the Magnetic Properties and Electrical Resistivity of $Fe_{73.5}Cu_1Nb_3Si_{13.5}B_9$ Nanocrystalline alloy. J Magn Magn Mater 1994;133:314-316.
10. Mondal SP, et al. Influence of Annealing Conditions on Nanocrystalline and Ultra-Soft Magnetic Properties of $Fe_{73.5}Cu_1Nb_3Si_{13.5}B_9$ alloy. J Mater Sci Technol 2012;28:21-26.
11. Hassiak M, et al. Effect of cooling rate on magnetic properties of amorphous and nanocrystalline $Fe_{73.5}Cu_1Nb_3Si_{13.5}B_9$ alloy. J Magn Magn Mater 2000;215-216:410-412.
12. Yoshizawa Y, et al. New Fe-based Soft Magnetic Alloys Composed of Ultra-fine Grains Structure. J Appl Phys 1988;64:6044-6046.
13. Cullity BD. Elements of X-Ray Diffraction. Addition Wesley, London 1959;262.
14. Franco V, et al. Changes in magnetic anisotropy distribution during structural evolution of $Fe_{76}Si_{10.5}B_{9.5}Cu_1Nb_3$. J Magn Magn Mater 1998;185:353-359.
15. Mondal SP, et al. Correlation between Structure and the magnetic properties of amorphous and nanocrystalline $Fe_{74}Cu_{0.5}Nb_3Si_{13.5}B_9$ alloys. J Bangladesh Acad Sci 2011;35:187-195.
16. Khalid Hossain Md, et al. Study and Characterization of Soft Magnetic Properties of $Fe_{73.5}Cu_1Nb_3Si_{13.5}B_9$ Magnetic Ribbon Prepared by Rapid Quenching Method. Mater Sci Appl 2015;06:1089-1099.
17. Phillips WA. Tunneling states in amorphous solids. J Low Temp Phys 1972;7:351-360.